J|A|C|S
ARTICLES
Published on Web 01/25/2006

Experimental and Computational Investigation of the Uncatalyzed Rearrangement and Elimination Reactions of Isochorismate

Michael S. DeClue,[†] Kim K. Baldridge,[‡] Peter Kast,[†] and Donald Hilvert*,[†]

Contribution from the Laboratory of Organic Chemistry, ETH Zürich, CH-8093 Zürich, Switzerland, and Organisch-Chemisches Institut, Universität Zürich, Winterthurerstrasse 190, CH-8057 Zürich, Switzerland

Received September 30, 2005; E-mail: hilvert@org.chem.ethz.ch

Abstract: The versatile biosynthetic intermediate isochorismate decomposes in aqueous buffer by two competitive pathways, one leading to isoprephenate by a facile Claisen rearrangement and the other to salicylate via elimination of the enolpyruvyl side chain. Computation suggests that both processes are concerted but asynchronous pericyclic reactions, with considerable C−O cleavage in the transition state but relatively little C−C bond formation (rearrangement) or hydrogen atom transfer to the enolpyruvyl side chain (elimination). Kinetic experiments show that rearrangement is roughly 8-times more favorable than elimination. Moreover, transfer of the C2 hydrogen atom to C9 was verified by monitoring the decomposition of [2-^{2}H]isochorismate, which was prepared chemoenzymatically from labeled shikimate, by ^{2}H NMR spectroscopy and observing the appearance of [3-^{2}H]pyruvate. Finally, the isotope effects obtained with the C2 deuterated substrate are in good agreement with calculations assuming pericyclic reaction mechanisms. These results provide a benchmark for mechanistic investigations of isochorismate mutase and isochorismate pyruvate lyase, the enzymes that respectively catalyze the rearrangement and elimination reactions in plants and bacteria.

A wide range of aromatic metabolites—including 6-hydroxyanthranilic acid, naphthoquinones, siderophores, 3-carboxy aromatic amino acids, and various plant epoxides— can be traced to isochorismate (**1**), a key branchpoint intermediate in the shikimate biosynthetic pathway.[1] The uncatalyzed decomposition of isochorismate has been previously investigated[2] and occurs via two competitive pathways, one leading to 3-carboxyphenylpyruvate (**3**), presumably via the intermediate isoprephenate (**2**), and the other to salicylate (**4**) and pyruvate (**5**) (Scheme 1). Nevertheless, scant attention has been paid to the mechanistic features of these transformations.

Here we describe a detailed experimental and computational study of the thermal decomposition of isochorismate. In addition to characterizing the reaction manifold kinetically, we have exploited selectively labeled [2-^{2}H]isochorismate (**1a**) to probe the nature of the competing transition states. Together with theoretical calculations, our data suggest that both elimination and rearrangement are concerted pericyclic processes with chairlike geometries. These findings provide a basis for understanding the mechanisms of the biosynthetic enzymes that act on isochorismate.

Materials and Methods

General Methods and Materials. All reactions were carried out in flame-dried glassware. THF was dried by distillation from sodium benzophenone ketyl. Methylene chloride was dried by distillation from CaH_2. All other chemicals and solvents were reagent grade and used as received. Chromatographic purifications were performed with Kieselgel 60, 230−400 mesh silica gel (Fluka). Eluent mixtures are reported as v/v percentages of the minor constituent in the major constituent. ^{1}H NMR spectra were referenced to dioxane ($C_4H_8O_2$) at 3.53 ppm in D_2O. ^{2}H NMR spectra were referenced to dioxane-d_8 ($C_4D_8O_2$) at 3.53 ppm in H_2O. All other spectra were referenced to the solvent. KA12/pKAD50/pKS3-02 was obtained by transforming the *Escherichia coli* strain KA12[3,4] with the plasmids pKAD50[5] and pKS3-02,[6] which confer choramphenicol and kanamycin resistance, respectively.

(3a*R*,4*S*,6*S*,6a*S*)-6-Benzyloxy-2,2-dimethyl-tetrahydro-furo[3,4-*d*][1,3]dioxole-4-carboxylic Acid (7). A solution of silver nitrate (20.4 g, 120 mmol) in H_2O (29.0 mL) was combined with benzyl 2,3-O-isopropylidene-α-D-lyxo-pentodialdo-1,4-furanoside (**6**)[7] (14.6 g, 52.3 mmol) dissolved in EtOH (290 mL). A solution of KOH (13.5 g, 240 mmol) in H_2O (290 mL) was added dropwise to the resulting mixture over 1.0 h. After the addition was complete, the reaction mixture was stirred at ambient temperature for an additional 1.5 h and then filtered to remove insoluble Ag_2O. The mother liquor was concentrated in vacuo to ca. 250 mL and then extracted with Et_2O (3 × 50 mL). The aqueous layer was separated, acidified to pH 2.0, and extracted again with Et_2O (3 × 150 mL). The combined Et_2O layers were dried over $MgSO_4$ and

[†] ETH Zürich.
[‡] Universität Zürich.

(1) Bentley, R. *Crit. Rev. Biochem. Mol. Biol.* **1990**, *25*, 307−384.
(2) Young, I. G.; Batterham, T. J.; Gibson, F. *Biochim. Biophys. Acta* **1969**, *177*, 389−400.
(3) Kast, P.; Asif-Ullah, M.; Hilvert, D. *Tetrahedron Lett.* **1996**, *37*, 2691−2694.
(4) Grisostomi, C.; Kast, P.; Pulido, R.; Huynh, J.; Hilvert, D. *Bioorg. Chem.* **1997**, *25*, 297−305.
(5) Dell, K. A.; Frost, J. W. *J. Am. Chem. Soc.* **1993**, *115*, 11581−11589.
(6) Schmidt, K.; Leistner, E. *Biotechnol. Bioeng.* **1995**, *45*, 285−291.
(7) Brimacombe, J. S.; Hunedy, F.; Tucker, L. C. N. *J. Chem. Soc. C* **1968**, 1381−1384.

10.1021/ja056714x CCC: $33.50

Scheme 1. Thermal Decomposition of Isochorismate

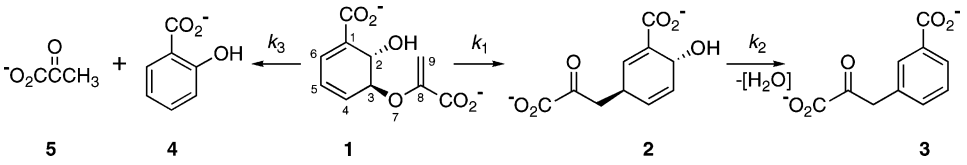

evaporated to yield 13.8 g (90%) of **7** as a white solid: mp 101−103 °C. ^{1}H NMR (300 MHz, $CDCl_3$): δ 1.32 (s, 3H), 1.46 (s, 3H), 4.53 (d, J = 11.7 Hz, 1H), 4.69−4.75 (m, 3H), 5.08 (dd, J = 5.9, 4.2 Hz, 1H), 5.30 (s, 1H), 7.27−7.39 (m, 5H), 9.29 (br s, 1H). ^{13}C NMR (75 MHz, $CDCl_3$): δ 24.8, 25.8, 69.4, 79.4, 80.4, 84.1, 105.7, 113.6, 128.0, 128.1, 128.5, 136.6, 171.8. HRMS-MALDI$^+$ (m/z): [M + Na]$^+$ calcd for $C_{15}H_{18}NaO_6$, 317.1001; found, 317.1001.

(3a*R*,4*S*,6*S*,6a*S*)-6-Benzyloxy-2,2-dimethyl-tetrahydro-furo[3,4-*d*][1,3]dioxole-4-carboxylic Acid Methyl Ester (8). Compound **7** (13.8 g, 47.1 mmol) was stirred with anhydrous MeOH (300 mL) and chlorotrimethylsilane (8.8 mL, 69.6 mmol) under nitrogen at ambient temperature for 3 h. The reaction was then treated with a dilute solution of ammonium hydroxide (1.0 mM, 50 mL) and concentrated in vacuo to ca. 50 mL. The residue was diluted with H_2O (50 mL) and extracted using Et_2O (3 × 125 mL). The combined Et_2O layers were dried over $MgSO_4$ and evaporated to yield 12.5 g of a light yellow oil. Purification by flash chromatography with silica absorbent (EtOAc/hexanes, 1:1) yielded 10.3 g (71%) of **8** as an off-white solid: mp 54−55 °C. ^{1}H NMR (300 MHz, $CDCl_3$): δ 1.29 (s, 3H), 1.43 (s, 3H), 3.82 (s, 3H), 4.50 (d, J = 11.7 Hz, 1H), 4.65−4.73 (m, 3H), 5.01 (dd, J = 6.0, 4.5 Hz, 1H), 5.28 (s, 1H), 7.27−7.37 (m, 5H). ^{13}C NMR (75 MHz, $CDCl_3$): δ 25.0, 25.9, 52.2, 69.3, 79.6, 80.5, 84.0, 105.5, 113.2, 127.8, 127.9, 128.3, 136.7, 167.6. HRMS-ESI$^+$ (m/z): [M + Na]$^+$ calcd for $C_{16}H_{20}NaO_6$, 331.1158; found, 331.1148.

((3a*S*,4*R*,6*S*,6a*S*)-6-Benzyloxy-2,2-dimethyl-tetrahydro-furo[3,4-*d*][1,3]dioxol-4-yl)-[di-^{2}H]methanol (9). A solution of **8** (15.7 g, 51 mmol) in dry THF (120 mL) was added dropwise over 30 min to a stirred suspension of lithium aluminum deuteride (2.14 g, 51 mmol) and THF (410 mL) at 0 °C under a flow of nitrogen. After the addition was complete the mixture was warmed to room temperature and stirred overnight. The reaction was then cooled to 0 °C, treated with a saturated aqueous solution of $MgSO_4$ (20 mL), and extracted using Et_2O (3 × 250 mL). The combined Et_2O layers were dried over $MgSO_4$ and evaporated to yield 13.3 g (93%) of **9** as a white solid. This material was used in the next step without further purification: mp 84−85 °C. ^{1}H NMR (300 MHz, $CDCl_3$): δ 1.31 (s, 3H), 1.47 (s, 3H), 2.25 (br s, 1H), 4.12 (d, J = 3.6 Hz, 1H), 4.50 (d, J = 12.0 Hz, 1H), 4.68 (d, J = 6.0 Hz, 1H), 4.70 (d, J = 11.4 Hz, 1H), 4.81 (dd, J = 6.2, 3.6 Hz, 1H), 5.15 (s, 1H), 7.27−7.39 (m, 5H). ^{13}C NMR (75 MHz, $CDCl_3$): δ 24.4, 25.8, 60.2 (pent, J = 21.8 Hz), 68.9, 79.4, 80.2, 85.1, 105.1, 112.6, 127.8, 128.0, 128.3, 137.2. HRMS-ESI$^+$ (m/z): [M + Na]$^+$ calcd for $C_{15}H_{18}D_2NaO_5$, 305.1332; found, 305.1326.

3-((3a*S*,4*R*,6*S*,6a*S*)-6-Benzyloxy-2,2-dimethyl-tetrahydro-furo-[3,4-*d*][1,3]dioxol-4-yl)-2-(diethoxy-phosphoryl)-[3,3-^{2}H$_2$]propionic Acid Methyl Ester (10). Triflic anhydride (9.8 mL, 58.2 mmol) was added dropwise over 10 min to a stirred solution of **9** (12.6 g, 44.6 mmol) in dry CH_2Cl_2 (125 mL) and pyridine (7.9 mL, 97.8 mmol) at −30 °C under a flow of nitrogen. After 15 min at −30 °C the reaction was quenched by the addition of H_2O (20 mL) and diluted with CH_2Cl_2 (150 mL). The CH_2Cl_2 layer was separated, washed with aqueous NaH_2PO_4 (1.0 M, 25 mL), dried over $MgSO_4$, and evaporated to afford 18.5 g (100%) of the triflate as a light pink oil. This intermediate is highly reactive and should be used as quickly as possibly. The crude triflate (18.5 g, 44.6 mmol) was dissolved in dry DMF (105 mL) and added to the ylid of methyl diethylphosphonoacetate, prepared in advance by adding methyl diethylphosphonoacetate (14.2 mL, 77.6 mmol) in dry DMF (70 mL) to a stirred suspension of sodium hydride (2.8 g, 69.7 mmol) in dry DMF (170 mL) at 0 °C. After addition of 15-crown-5 (5 drops), the mixture was stirred overnight at room temperature to furnish a dark solution. The reaction was subsequently cooled to 0 °C, quenched with aqueous NaH_2PO_4 (1.0 M, 100 mL), and then extracted with $CHCl_3$ (3 × 300 mL). The combined $CHCl_3$ layers were washed with H_2O (25 mL), dried over $MgSO_4$, and evaporated to yield a red oil. Purification by flash chromatography with silica absorbent (EtOAc/hexanes, 1:1) afforded 21.0 g (99%) **10** as a mixture of diastereomers. ^{1}H NMR (300 MHz, $CDCl_3$): δ 1.27−1.37 (m, 18H), 1.42 (s, 3H), 1.43 (s, 3H), 3.16 (d, J = 22.8 Hz, 1H), 3.38 (d, J = 22.8 Hz, 1H), 3.72 (s, 3H), 3.76 (s, 3H), 4.07−4.24 (m, 10H), 4.34−4.68 (m, 8H), 5.00 (s, 1H), 5.01 (s, 1H), 7.27−7.40 (m, 10H). ^{13}C NMR (75 MHz, $CDCl_3$): δ 16.1, 16.2, 24.8, 24.9, 25.9 (br s), 42.1 (d, J = 131 Hz), 42.6 (d, J = 131 Hz), 52.4 (br s), 62.6−62.9 (m), 68.3, 68.6, 78.1, 78.3, 79.8, 80.2, 85.2, 85.4, 104.4, 104.8, 112.5 (br s), 127.7, 127.9, 128.0, 128.1, 128.4, 128.5, 137.1 (br s), 169.4, 169.5. ^{31}P NMR (121.5 MHz, $CDCl_3$): δ 22.69, 22.95. HRMS-ESI$^+$ (m/z): [M + Na]$^+$ calcd for $C_{22}H_{31}D_2NaO_9P$, 497.1883; found, 497.1871.

2-(Diethoxy-phosphoryl)-[3,3-^{2}H$_2$]-3-((3a*S*,4*R*,6*S*,6a*S*)-6-hydroxy-2,2-dimethyl-tetrahydro-furo[3,4-*d*][1,3]dioxol-4-yl)-propionic Acid Methyl Ester (11). Compound **10** (21.0 g, 44.2 mmol) was dissolved in methanol (630 mL), and stirred with H_2O (32 mL), ammonium formate (26.5 g, 420 mmol), and 10% Pd/C (14.0 g) at 50 °C for 1 h. After cooling to room temperature and filtering off the Pd/C, the solution was evaporated under reduced pressure to yield an oily white solid. The residue was suspended in EtOAc (400 mL) and filtered to remove insoluble contaminants. The EtOAc solution was then dried over $MgSO_4$ and evaporated to afford 16.8 g (99%) of **11** as a mixture of diastereomers. This material was used in the next step without further purification. ^{1}H NMR (300 MHz, $CDCl_3$): δ 1.19−1.27 (m, 18H), 1.33 (s, 3H), 1.34 (s, 3H), 3.07 (d, J = 22.8 Hz, 1H), 3.14 (d, J = 22.8 Hz, 1H), 3.64 (s, 6H), 3.96−4.12 (m, 10H), 4.45−4.55 (m, 4H), 5.19 (s, 2H). ^{13}C NMR (75 MHz, $CDCl_3$): δ 16.1 (br s), 24.6, 24.7, 25.7, 25.8, 41.8 (d, J = 131 Hz), 52.3 (br s), 62.5−62.8 (m), 79.6 (br s), 80.3 (br s), 85.7, 85.9, 100.3, 100.4, 112.1 (br s), 169.2 (br s). ^{31}P NMR (121.5 MHz, $CDCl_3$): δ 22.72, 23.17. HRMS-ESI$^+$ (m/z): [M + Na]$^+$ calcd for $C_{15}H_{25}D_2NaO_9P$, 407.1414; found, 407.1405.

Methyl 3,4-O-Isopropylidene[6,6-^{2}H$_2$]shikimate (12). A solution of **11** (6.63 g, 17.3 mmol) in dry methanol (100 mL) was added dropwise to a precooled solution of sodium methoxide, which was prepared by adding dry methanol (200 mL) to sodium (1.3 g, 56.2 mmol, washed once with hexanes) over 30 min under a flow of nitrogen while maintaining the temperature at 0 °C. The mixture was then warmed to room temperature and stirred for 2 h. The reaction was quenched by addition of a saturated aqueous solution of $NaHCO_3$ (350 mL) and extracted with Et_2O (3 × 500 mL). The combined Et_2O layers were washed with saturated aqueous NaCl (50 mL), dried over $MgSO_4$, and evaporated to provide 2.4 g of a light yellow oil. Purification by flash chromatography with silica absorbent (EtOAc/hexanes, 3:7) yielded 1.2 g (31%) of **12** as a clear oil. ^{1}H NMR (300 MHz, $CDCl_3$): δ 1.41 (s, 3H), 1.45 (s, 3H), 2.22 (br s, 1H), 3.78 (s, 3H), 3.89 (d, J = 7.5 Hz, 1H), 4.09 (apparent t, J = 7.5 Hz, 1H), 4.75 (dd, J = 6.2, 3.6 Hz, 1H), 6.93 (d, J = 3.6 Hz, 1H). ^{13}C NMR (75 MHz, $CDCl_3$): δ 25.7, 27.9, 28.6 (pent, J = 20.0 Hz), 52.1, 68.5, 72.2, 77.8, 109.6, 130.4, 134.0, 166.6. HRMS-ESI$^+$ (m/z): [M + Na]$^+$ calcd for $C_{11}H_{14}D_2NaO_5$, 253.1019; found, 253.1013.

Methyl [6,6-^{2}H$_2$]Shikimate (13). Compound **12** (950 mg, 4.1 mmol) was mixed with Dowex-50WX8-200 (1.6 g, washed with methanol three times and dried under vacuum for 30 min) in methanol (100 mL)

containing 5.8 mL of H_2O. The mixture was stirred overnight at room temperature under an atmosphere of nitrogen. The solution was then filtered and the resin washed with methanol (3 × 5 mL). The combined methanol layers were evaporated to afford 870 mg of a light yellow solid. Purification by flash chromatography with silica absorbent ($MeOH/CH_2Cl_2$, 1:9) yielded 720 mg (92%) of **13** as a white solid: mp 113.5−114.5 °C. ^1H NMR (300 MHz, CD_3OD): δ 3.68 (dd, J = 7.2, 3.9 Hz, 1H), 3.73 (s, 3H), 3.98 (d, J = 6.9 Hz, 1H), 4.37 (apparent t, J = 3.9 Hz, 1H), 6.78 (d, J = 3.6 Hz, 1H). ^{13}C NMR (75 MHz, CD_3OD): δ 30.8 (pent, J = 20.0 Hz), 52.4, 67.2, 68.2, 72.5, 130.1, 139.1, 168.7. HRMS-ESI$^+$ (m/z): $[M + Na]^+$ calcd for $C_8H_{10}D_2NaO_5$, 213.0706; found, 213.0700.

Preparation of the Crude Cell Extract from *E. coli* Strain KA12/pKAD50/pKS3-02. A 500 mL Erlenmeyer flask supplied with Miller's LB broth[8] (100 mL) was sterilized by autoclaving. After cooling, the broth was supplemented with solutions of kanamycin sulfate in H_2O (15 mg/mL, 200 μL), chloramphenicol in EtOH (30 mg/mL, 200 μL), tryptophan in H_2O (8 mg/mL, 500 μL), and ammonium ferrous sulfate in H_2O (5 mM, 200 μL), and then inoculated with a single colony of *E. coli* strain KA12[3,4] transformed with plasmids pKAD50[5] and pKS3-02.[6] This preculture was shaken at 230 rpm for 24 h at 37 °C (final OD = 2.2 at 600 nm). Six 3 L Erlenmeyer flasks, each containing Miller's LB broth (1.0 L), kanamycin sulfate (30 mg), chloramphenicol (60 mg), tryptophan (40 mg), and an aliquot of a freshly prepared aqueous solution of ammonium ferrous sulfate (5 mM, 2.0 mL) were each inoculated with 15 mL of the KA12/pKAD50/pKS3-02 preculture. The cultures were shaken at 230 rpm for 24 h at 37 °C (final OD = 3.8 at 600 nm). After cooling to room temperature, cells were collected by centrifugation at 5000 rpm (4200*g*; 15 min, 4 °C). The cell pellet was resuspended in Tris−HCl (50 mM, pH 8.0) containing DL-dithiothreitol (DTT, 1.0 mM). Recentrifugation at 5000 rpm (4200*g*; 15 min, 4 °C) yielded 33 g of cells. The cell pellet was suspended in Tris−HCl (120 mL, 50 mM, pH 8.0) containing DTT (1.0 mM), and the cells were ruptured by passage through a French press (three times). Cell debris was removed from the lysate by centrifugation at 10 000 rpm (16 420*g*; 30 min, 4 °C). The supernatant was initially dialyzed at 4 °C against Tris−HCl (2.0 L, 50 mM, pH 8.0) containing DTT (1.0 mM) and a solution of phenylmethanesulfonyl fluoride (50 mg PMSF dissolved in 1.0 mL of CH_3CN) and then exhaustively in the same buffer lacking PMSF. It was stored at 4 °C prior to use. *Note: best yields of isochorismate in the following procedures were obtained with freshly prepared cell extract.*

Isochorismate (1). The monosodium salt of ATP (2.28 g, 4.14 mmol) was added in portions to Tris−HCl (95 mL, 50 mM, pH 8.0) while maintaining the pH of the solution between 6.5 and 9.0. To this solution were added FMN (140 mg, 0.28 mmol), the monopotassium salt of phosphoenolpyruvate (1.72 g, 8.33 mmol), a solution of KCl (1.0 M aqueous, 6.9 mL, 6.9 mmol), a solution of $MgSO_4$ (1.0 M aqueous, 0.69 mL, 0.69 mmol), and shikimic acid (480 mg, 2.76 mmol). KA12/pKAD50/pKS3-02 extract (35 mL, corresponding to a lysate fraction originating from ca. 10 g of cells with an estimated total protein concentration of ca. 40 mg/mL) was added, and the pH of the resulting mixture was adjusted to 8.0 using NaOH (10.0 N). After addition of sodium dithionite (270 mg, 1.56 mmol), the reaction mixture was sealed and gently stirred at 23 °C for 1 h. It was then brought rapidly to about 0 °C and filtered through an Amicon ultrafiltration membrane (10 K cutoff) at 4 °C, while cooling the collected filtrate in a slurry of ice and NaCl. When nearly dry, the membrane was washed with Tris−HCl (20 mL, 50 mM, pH 8.0). The combined filtrate was acidified to pH 1.5 and extracted with EtOAc (6 × 100 mL). The combined extracts were dried over Na_2SO_4 and carefully concentrated in vacuo (maintaining the rotary evaporator bath at ca. 15 °C). The resulting light yellow oil was purified by preparative reverse phase HPLC (Macherey-Nagel Nucleosil 100-7 C-18 VP 250/21, CH_3CN/H_2O containing 0.1% TFA, linear gradient from 5% to 40% CH_3CN over 40 min, total flow rate of 10 mL/min) to give isochorismic acid (retention time 21.7 min) and chorismic acid (retention time 23.9 min). The corresponding fractions were lyophilized, affording isochorismic acid (37 mg, 6%) as a white solid and chorismic acid (55 mg, 9%) as an off-white solid. The ^1H NMR spectra of chorismic acid[9] (not reported) and isochorismic acid[10] match published data. ^1H NMR (300 MHz, DMSO-d_6): δ 4.47 (bs s, 1H), 4.53 (d, J = 4.7 Hz, 1H), 4.96 (br s, 1H), 5.31 (br s, 1H), 6.24 (dd, J = 9.3, 4.7 Hz, 1H), 6.35 (dd, J = 9.3, 5.4 Hz, 1H), 6.96 (d, J = 5.4 Hz, 1H). ^1H NMR (300 MHz, D_2O, pD 7.5, 60 °C): δ 4.49 (d, J = 2.4 Hz, 1H), 4.54 (d, J = 4.8 Hz, 1H), 4.61 (d, J = 5.1 Hz, 1H), 5.01 (d, J = 2.4 Hz, 1H), 5.98 (ddd, J = 9.6, 4.4, 1.2 Hz, 1H), 6.12 (ddd, J = 9.6, 5.6, 1.2 Hz, 1H), 6.59 (d, J = 5.6, 1.2 Hz, 1H).

[2-^{2}H]Isochorismate (1a). Compound **13** (525 mg, 2.76 mmol) was dissolved in a mixture of THF (20.5 mL), H_2O (17.6 mL), and NaOH (1 M, 2.9 mL, 2.9 mmol). The solution was stirred at 23 °C for 3 h. After the removal of THF by distillation in vacuo, the aqueous mixture was lyophilized to yield 545 mg of the labeled sodium shikimate as a white solid. Using the conditions described above for isochorismate (**1**), the crude sodium [6,6-$^2H_2$]shikimate (545 mg, 2.76 mmol) was converted chemoenzymatically into [2-^{2}H]chorismate (46 mg, 7%) and **1a** (49 mg, 8%). [2-^{2}H]Chorismate. ^1H NMR (300 MHz, CD_3OD): δ 4.69 (dt, J = 11.4, 2.7 Hz, 1H), 4.82 (d, J = 3.0 Hz, 1H), 4.94 (d, J = 11.4 Hz, 1H), 5.49 (d, J = 3.0 Hz, 1H), 5.99 (ddd, J = 10.1, 2.4, 0.9 Hz, 1H), 6.34 (dd, J = 10.1, 2.7 Hz, 1H). [2-^{2}H]Isochorismate. ^1H NMR (300 MHz, DMSO-d_6): δ 4.53 (d, J = 4.2 Hz, 1H), 4.82 (br s, 1H), 5.24 (br s, 1H), 6.18 (dd, J = 9.5, 4.2 Hz, 1H), 6.30 (dd, J = 9.5, 4.5 Hz, 1H), 6.88 (d, J = 4.5 Hz, 1H). ^1H NMR (300 MHz, D_2O, pD 7.5, 60 °C): δ 4.49 (d, J = 2.8 Hz, 1H), 4.52 (d, J = 4.5 Hz, 1H), 5.01 (d, J = 2.8 Hz, 1H), 5.98 (ddd, J = 9.6, 4.4, 1.2 Hz, 1H), 6.13 (ddd, J = 9.6, 5.6, 1.2 Hz, 1H), 6.59 (dd, J = 5.6, 1.2 Hz, 1H). ^2H NMR (61.4 MHz, H_2O, pH 6.0, 60 °C): δ 4.64 (br s, 1^{2}H).

NMR Kinetics. The reaction of isochorismate and [2-^{2}H]isochorismate (20 mM) was monitored at 60 °C by ^1H NMR spectroscopy in deuterated phosphate buffer (200 mM, pD 7.5) containing dioxane (1.0 mM) as an internal standard. The concentrations of isochorismate, isoprephenate, 3-carboxyphenylpyruvate, salicylate, and pyruvate were determined periodically by integration of representative, well-resolved peaks and comparison to the internal standard. The kinetic data were analyzed with the program DynaFit.[11] The decomposition of [2-^{2}H]-isochorismate in phosphate buffer (200 mM, pH 6.0, 60 °C) was similarly monitored by ^2H NMR spectroscopy using dioxane-d_8 as the internal standard. All experiments were performed in duplicate. Isoprephenate (**2**). ^1H NMR (300 MHz, D_2O, pD 7.5, 60 °C): δ 2.57−2.75 (m, 2H), 3.13−3.21 (m, 1H), 4.70−4.75 (m, 1H), 5.72−5.76 (m, 2H), 6.42 (d, J = 2.7 Hz, 1H). [4-^{2}H]Isoprephenate. ^1H NMR (300 MHz, D_2O, pD 7.5, 60 °C): δ 2.57−2.75 (m, 2H), 3.13−3.22 (m, 1H), 5.73−5.76 (m, 2H), 6.42 (d, J = 3.3 Hz, 1H). ^2H NMR (61.4 MHz, H_2O, pH 6.0, 60 °C): δ 4.75 (br s, 1^{2}H). 3-Carboxyphenylpyruvate (**3**). ^1H NMR (300 MHz, D_2O, pD 7.5, 60 °C): δ 3.17 (s, 2H), 7.14−7.26 (m, 2H), 7.47−7.63 (m, 2H). 3-Carboxy[4-^{2}H]phenylpyruvate. ^1H NMR (300 MHz, D_2O, pD 7.5, 60 °C): δ 3.18 (s, 2H), 7.16 (dd, J = 7.7, 2.0 Hz, 1H), 7.24 (d, J = 7.8 Hz, 1H), 7.48 (d, J = 2.0 Hz, 1H). ^2H NMR (61.4 MHz, H_2O, pH 6.0, 60 °C): δ 7.65 (br s, 1^{2}H). Salicylate (**4**). ^1H NMR (300 MHz, D_2O, pD 7.5, 60 °C): δ 6.72−6.79 (m, 2H), 7.21−7.27 (m, 1H), 7.62 (dd, J = 7.7, 1.7 Hz, 1H). Pyruvate (**5**). ^1H NMR (300 MHz, D_2O, pD 7.5, 60 °C): δ 2.14 (s, 3H). [3-^{2}H]Pyruvate. ^1H NMR (300 MHz, D_2O, pD 7.5, 60 °C): δ 2.13 (t, J = 2.4 Hz, 2H). ^2H NMR (61.4 MHz, H_2O, pH 6.0, 60 °C): δ 2.19 (br s, 1^{2}H).

Computational Studies. All calculations were performed using the GAMESS[12] and GAUSSIAN[13] series of programs. Both hybrid density

(8) Miller, J. H. *A Short Course in Bacterial Genetics. A Laboratory Manual and Handbook for Escherichia coli and Related Bacteria*; Cold Spring Harbor Laboratory: Cold Spring Harbor, NY, 1992.

(9) Copley, S. D.; Knowles, J. R. *J. Am. Chem. Soc.* **1987**, *109*, 5008−5013.
(10) Gould, S. J.; Eisenberg, R. L. *Tetrahedron* **1991**, *47*, 5979−5990.
(11) Kuzmic, P. *Anal. Biochem.* **1996**, *237*, 260−273.

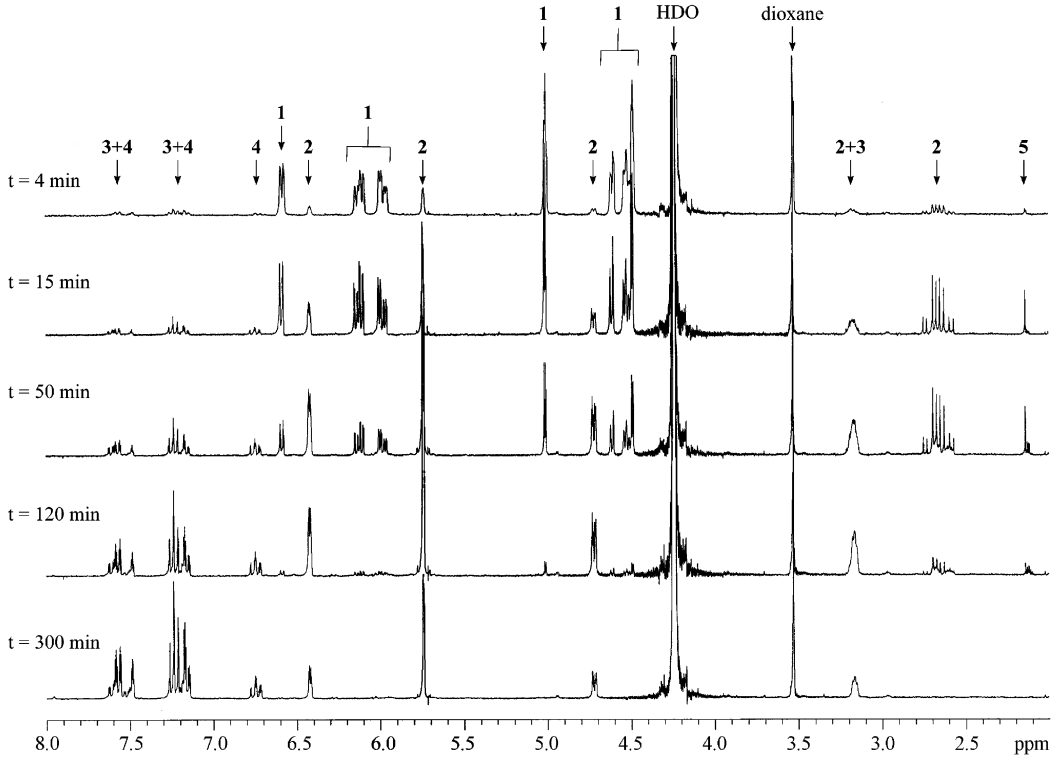

Figure 1. ^{1}H NMR spectroscopic analysis of the nonenzymatic decomposition of isochorismate (20 mM) at 60 °C in 200 mM sodium phosphate buffer in D_2O (pD 7.5) with 1.0 mM dioxane as an internal standard. The signals associated with isochorismate (**1**), isoprephenate (**2**), 3-carboxyphenylpyruvate (**3**), salicylate (**4**), and pyruvate (**5**) are indicated.

functional (B3LYP)[14] and Møller−Plesset 2 (MP2)[15] theories were considered, using the DZ+(2d,p) basis set.[16] Only the former are presented here since no substantial differences were found. Full geometry optimizations were performed and uniquely characterized by calculating and diagonalizing the matrix of energy second derivatives (Hessian) to determine the number of imaginary frequencies (0 = minima; 1 = transition state). All results include zero-point corrections. Effects of solvent were considered using the self-consistent polarized continuum model COSMO.[17] Isotope effects were calculated by harmonic frequency analysis using QUIVER[18] with a frequency scaling factor of 0.961, a temperature of 333 K, and infinite parabola (KIE/ip tunneling corrections.[19] The diequatorial substrate conformer of isochorismate served as the reference state (see the Supporting Information).

Results

Kinetics. The thermal decomposition of isochorismate is readily monitored by ^{1}H NMR spectroscopy. As shown in Figure 1, the reaction proceeds cleanly at 60 °C in 200 mM sodium phosphate buffer in D_2O (pD 7.5) to produce isoprephenate (**2**), 3-carboxyphenylpyruvate (**3**), which arises from further reaction of isoprephenate, salicylate (**4**) and pyruvate (**5**). A typical time course for the disappearance of substrate and for the appearance of the individual products is shown in Figure 2A. The calculated rate constants for each step of this process (Scheme 1) are $k_1 = (3.63 \pm 0.09) \times 10^{-4}$ s^{-1}, $k_2 = (5.44 \pm 0.01) \times 10^{-5}$ s^{-1}, and $k_3 = (4.65 \pm 0.22) \times 10^{-5}$ s^{-1}. Under the experimental conditions, the pyruvate that is produced in the elimination step also exchanges with solvent with an apparent rate constant of $k_4 = (3.93 \pm 0.64) \times 10^{-4}$ s^{-1}. As seen from the k_1/k_3 ratio, rearrangement is more favorable than elimination by a factor of ca. 8. For comparison, k_1/k_3 was previously reported to be about 4 at 100 °C, based on salicylate concentrations estimated by fluorescence measurements.[2]

[2-^{2}H]Isochorismate Synthesis and Reactivity. To gain further insight into the elimination reaction, [2-^{2}H]isochorismate (**1a**) was prepared chemoenzymatically. As shown in Scheme 2, [6,6-$^2H_2$]shikimic acid was synthesized chemically and converted enzymatically to the selectively labeled isochorismate derivative.

The required shikimate derivative (**13**) was prepared from aldehyde **6**, which was obtained in four steps from D-mannose.[20] Mild oxidation with Ag_2O gave carboxylic acid **7**, which was converted to methyl ester **8**. The deuterium label was then introduced by reducing **8** with $LiAlD_4$. Activation of the primary alcohol **9** as a triflate, followed by substitution with methyl diethylphosphonoacetate, provided **10** in nearly quantitative yield over two steps. After removing the benzyl ether, compound **11** was converted to shikimate derivative **12** via an intramolecular Horner−Wadsworth−Emmons reaction. Subsequent

(12) Schmidt, M. W.; Baldridge, K. K.; Boatz, J. A.; Elbert, S. T.; Gordon, M. S.; Jensen, J. H.; Koseki, S.; Matsunaga, N.; Nguyen, K. A.; Su, S. J.; Windus, T. L.; Dupuis, M.; Montgomery, Jr., J. A. *J. Comput. Chem.* **1993**, *14*, 1347−1363.
(13) Frisch, M. J.; et al. *Gaussian03*, revision C.01; Gaussian, Inc.: Wallingford, CT, 2004.
(14) Becke, A. D. *J. Chem. Phys.* **1993**, *98*, 5648−5652.
(15) Møller, C.; Plesset, M. S. *Phys. Rev.* **1934**, *46*, 618−622.
(16) Dunning, Jr., T. H.; Hay, P. J. In *Modern Theoretical Chemistry*; Schaefer, III, H. F., Ed.; Plenum: New York, 1976; Vol. 3, pp 1−27.
(17) (a) Klamt, A.; Schüürmann, G. *J. Chem. Soc., Perkin Trans. 2* **1993**, 799−805. (b) Baldridge, K. K.; Klamt, A. *J. Chem. Phys.* **1997**, *106*, 6622−6633.
(18) Saunders, M.; Laidig, K. E.; Wolfsberg, M. *J. Am. Chem. Soc.* **1989**, *111*, 8989−8994.
(19) Bell, R. P. *The Tunnel Effect in Chemistry*; Chapman and Hall: New York, 1980; pp 60−63.
(20) (a) Fleet, G. W. J.; Shing, T. K. M. *Chem. Commun.* **1983**, 849−850. (b) Fleet, G. W. J.; Shing, T. K. M.; Warr, S. M. *J. Chem. Soc., Perkin Trans. 1* **1984**, 905−908.

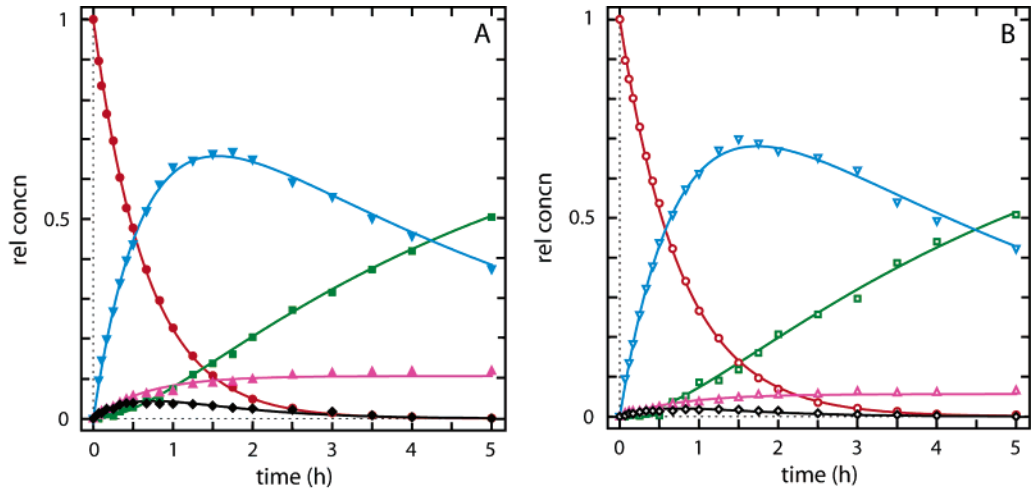

Figure 2. Kinetic analysis of the nonenzymatic decomposition of isochorismate (A) and [2-^{2}H]isochorismate (B) in 200 mM phosphate buffer in D_2O at 60 °C. The reactions were monitored by ^{1}H NMR spectroscopy. Relative concentrations of isochorismate (red circles), isoprephenate (blue inverted triangles), 3-carboxyphenylpyruvate (green squares), salicylate (magenta triangles), and pyruvate (black diamonds) are plotted as a function of time. The data were analyzed with the program DynaFit (ref 11).

Scheme 2. Synthesis of [2-^{2}H]isochorismate (**1a**)[a]

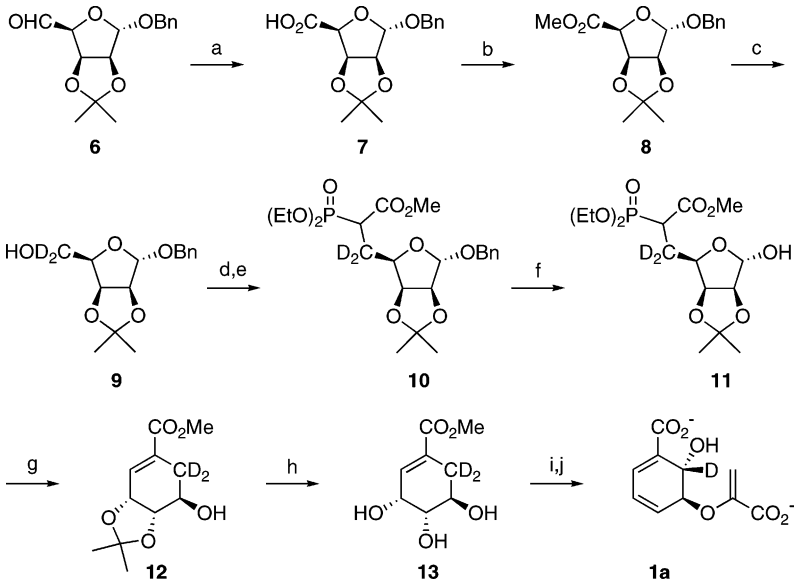

[a] Conditions: (a) $AgNO_3$, KOH, EtOH, H_2O, 90%; (b) $(CH_3)_3SiCl$, MeOH, 71%; (c) $LiAlD_4$, THF, 0 °C, 93%; (d) $(CF_3SO_2)_2O$, py, CH_2Cl_2, −30 °C; (e) $(EtO)_2P(O)CH_2CO_2Me$, NaH, DMF, 99% over two steps; (f) Pd/C, MeOH, HCO_2NH_4, 50 °C, 99%; (g) MeOH, Na^0, 0 °C, 31%; (h) Dowex 50WX8-200, MeOH, H_2O, 92%; (i) NaOH, THF, H_2O; (j) KA12/pKAD50/pKS3-02, Tris−HCl (pH 8.0), PEP, ATP, FMN, KCl, $MgSO_4$, NaS_2O_4, 8% over two steps.

acid-catalyzed hydrolysis of the isopropylidene ketal with Dowex 50W-X8 resin gave methyl [6,6-$^2H_2$]shikimate **13**, which afforded selectively labeled sodium shikimate upon saponification.

For the enzymatic transformation of shikimate, we modified a previously engineered *E. coli* strain, KA12/pKAD50, which overproduces the biosynthetic enzymes shikimate kinase, EPSP synthase, and chorismate synthase and efficiently converts shikimate to chorismate.[21] Transformation of KA12/pKAD50 with plasmid pKS3-02,[6] which carries the *entC* gene encoding isochorismate synthase, enables further metabolism of chorismate to isochorismate. Incubating crude sodium shikimate and phosphoenolpyruvate (PEP) with cell extracts from KA12/pKAD50/pKS3-02 for 1 h at 23 °C produces an equilibrium mixture of unlabeled chorismate and isochorismate in a ca. 3:2 ratio. Extraction of the crude reaction mixture and purification by preparative reversed-phase HPLC[4] affords milligram amounts of both compounds. In the same way, roughly 50 mg of [2-^{2}H]-isochorismate was obtained from 545 mg of methyl [6,6-$^2H_2$]-shikimate, corresponding to an overall yield of 8%.

The KA12/pKAD50/pKS3-02 production strain represents an attractive alternative to a recombinant strain of *Klebsiella pneumoniae* 62-1, a class 2 pathogenic organism, which has been used previously to produce isochorismate.[6] The combined yield of chorismate and isochorismate (about 15%) is substantially lower than the ca. 50% yield of chorismate previously observed for the KA12/pKAD50 system,[21] presumably due to the relative instability of isochorismate and its continuous metabolic depletion in the cell extract. Nevertheless, preparatively useful quantities of selectively labeled isochorismate derivatives can be easily produced.

(21) Gustin, D. J.; Hilvert, D. *J. Org. Chem.* **1999**, *64*, 4935−4938.

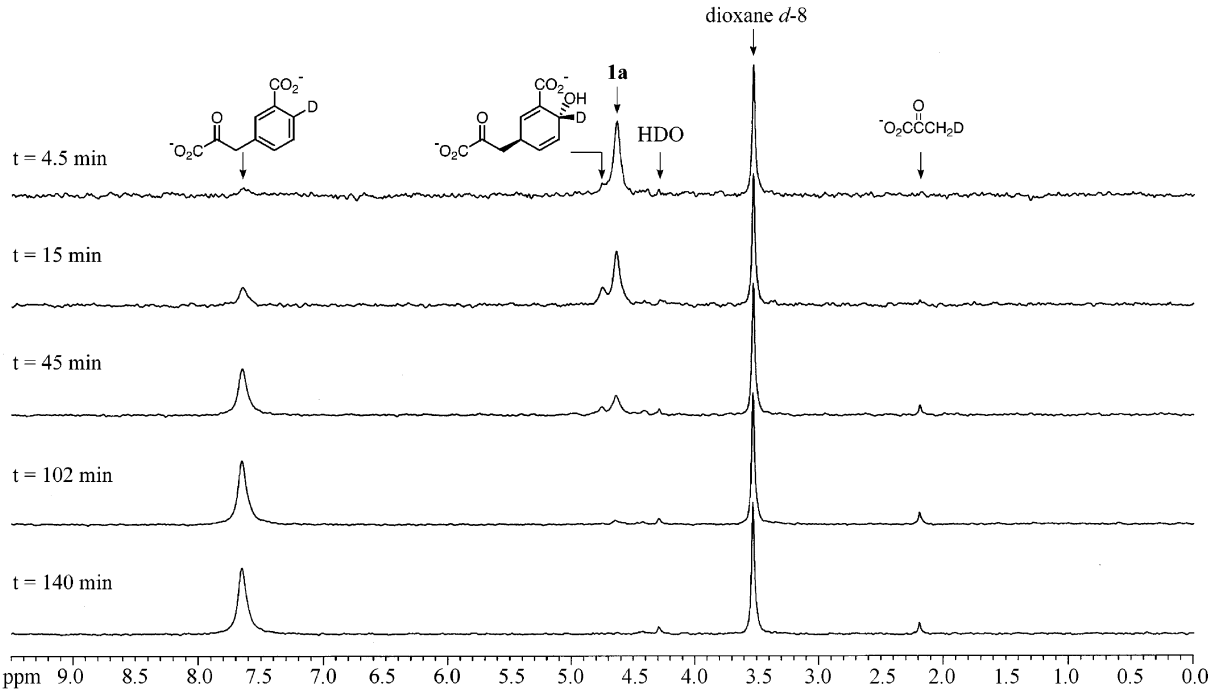

Figure 3. Decomposition of [2-^{2}H]isochorismate (**1a**) in 200 mM phosphate buffer (pH 6.0 and 60 °C) monitored by ^{2}H NMR spectroscopy. Dioxane-d_8 (1.00 mM) was used as an internal standard.

The effect of deuterium substitution at C2 on the reaction manifold was determined by monitoring the decomposition of [2-^{2}H]isochorismate at 60 °C by ^{1}H NMR as described for the unlabeled compound. A representative time course is shown in Figure 2B. The rate constants derived for the rearrangement, aromatization, and elimination steps are $k_1 = (3.43 \pm 0.01) \times 10^{-4}$ s^{-1}, $k_2 = (5.37 \pm 0.14) \times 10^{-5}$ s^{-1}, and $k_3 = (2.03 \pm 0.02) \times 10^{-5}$ s^{-1}, respectively. Comparison with the corresponding kinetic constants obtained with unlabeled isochorismate gives deuterium isotope effects of 1.06 ± 0.03, 1.01 ± 0.03, and 2.29 ± 0.11 on the k_1, k_2, and k_3 steps.

The fate of the deuterium atom at C2 during decomposition of [2-^{2}H]isochorismate was established by ^{2}H NMR spectroscopy at 60 °C (Figure 3). A pH of 6.0 was chosen for these experiments to minimize exchange with solvent. In agreement with the kinetic data (Figure 2B), both [4-^{2}H]isoprephenate and 3-carboxy[4-^{2}H]phenylpyruvate, which derive from the energetically more favorable rearrangement pathway, are readily detected by the characteristic signal of their single deuterium atom. In addition, sizable amounts of [3-^{2}H]pyruvate, which arises from the minor elimination pathway, are also observed. Roughly 70% of the pyruvate formed within 3 h contains deuterium originating from C2 of the labeled isochorismate as judged from direct integration of the respective signals for deuterated and deuterium-free pyruvate observed by ^{1}H NMR spectroscopy after lyophilization of the NMR sample. Given the observed rate of exchange under the experimental conditions, formation of unlabeled pyruvate can be entirely explained by direct exchange of [3-^{2}H]pyruvate with solvent.

Computation. Isochorismate is a flexible molecule. HDFT calculations at the B3LYP/DZ+(2d,p) level of theory show that pseudodiequatorial conformations, which are stabilized by an intramolecular hydrogen bond between the C1 carboxylate group and the C2 alcohol, are lowest in energy (Figure 4, left); the enolpyruvyl side chain is not particularly constrained, however,

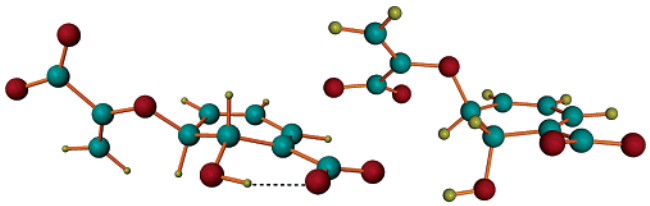

Figure 4. Pseudodiequatorial (left) and pseudodiaxial (right) conformation of isochorismate (**1**) (B3LYP/DZ+(2d,p)). The O−C2−C3−O dihedral angle for these structures is 77.2° and 141.0°, respectively.

and can easily adopt multiple orientations with minimal energetic penalty. In contrast, pseudodiaxial conformers, in which the hydrogen bond between the C1 carboxylate and the C2 alcohol is broken (Figure 4, right), are substantially higher in energy. In the gas phase, the latter are at least 10.1 kcal/mol less stable than the lowest energy pseudodiequatorial conformer. The calculated difference drops to 8.0 kcal/mol when the two carboxylate groups are shielded in a dielectric continuum that mimics water,[17] but this large value makes it unlikely that pseudodiaxial conformers are significantly populated in solution.

The conversion of isochorismate to isoprephenate is formally a [3,3]-sigmatropic rearrangement, and two different aromatic transition structures, corresponding to chairlike and boatlike geometries, respectively, were located at the B3LYP/DZ+(2d,p) level of theory (Figure 5). Both are highly asymmetric, with C−O bond cleavage significantly preceding C−C bond formation. The O−C2−C3−O dihedral angles in these structures (138° for the chair and 126° for the boat) approach that of the pseudodiaxial ground state conformer (141°), suggesting that substrate must undergo an unfavorable conformational change prior to rearrangement that contributes significantly to the overall reaction barrier. The calculated activation energy for rearrangement via the boat transition state is 26.5 kcal/mol, in reasonable agreement with the experimental value of 24.8 kcal/mol (Table 1). However, agreement between theory and experiment is poor

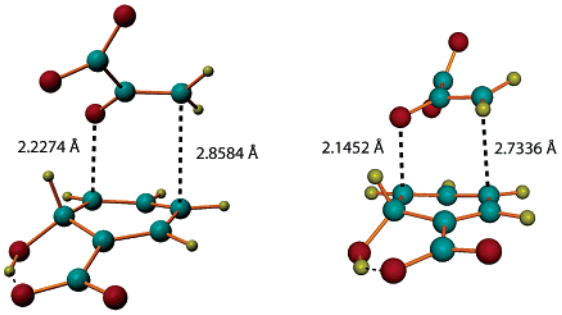

Figure 5. Chairlike (left) and boatlike (right) transition structures for the [3,3]-sigmatropic rearrangement of isochorismate to isoprephenate (B3LYP/DZ+(2d,p)). These structures have an O−C2−C3−O dihedral angle of 138.0° and 126.3°, respectively.

Table 1. Calculated Activation Energies and Isotope Effects for the Thermal Decomposition of Isochorismate at 333.15 K

reaction	E_a (kcal/mol)[a]	$E_{a\text{-Solution}}$ (kcal/mol)[a]	^{2}H KIE[b]
Claisen TS1 (chair)	35.8	24.9	1.027
Claisen TS2 (boat)	26.5	26.2	0.989
elimination TS1 (chair)	25.0	22.0	2.071
elimination TS2 (twist boat)	26.4	24.8	1.830

[a] Delta energy difference between the transition state indicated and the pseudoequatorial ground state conformation. For comparison, the experimental activation energies for the Claisen rearrangement and the elimination reaction are 24.8 and 26.2 kcal/mol, respectively, at this temperature. [b] Kinetic isotope effects (KIE) calculated for [2-^{2}H]isochorismate. For comparison, the experimental values for the Claisen rearrangement and the elimination reaction are 1.06 ± 0.03 and 2.29 ± 0.11, respectively, at T = 333.15 K, as described in the text.

for the ^{2}H isotope effect at C2 (predicted, 0.989; observed, 1.06 ± 0.03). In contrast, the chairlike transition state predicts a normal isotope effect of 1.027 that is much closer to the observed value, but the barrier in this case is unrealistically high (35.8 kcal/mol) (Table 1). Chairlike transition states are usually favored for Claisen rearrangements,[22] but in isochorismate juxtaposition of the negatively charged carboxylates greatly destabilizes the chair relative to the boat in the gas phase. Consistent with this explanation, when the charges are shielded in a dielectric continuum to model an aqueous environment,[17] rearrangement via the chair is predicted to be favored over the boat by 1.3 kcal/mol (Table 1).

The isochorismate elimination reaction can also be described as a pericyclic process, i.e., a [1,5]-sigmatropic rearrangement in which the C−O bond is cleaved simultaneously with hydrogen atom transfer from C2 to C9. Again, two conformationally distinct transition state structures were located, which differ in energy by 1.4 kcal/mol in the gas phase (Figure 6; Table 1). The more favorable has a chairlike geometry, with the carboxylate on the side chain directed over the ring, whereas the higher energy structure is better described as a twist boat in which the side chain carboxylate is directed away from the ring. As in the case of the Claisen rearrangement, both elimination transition structures correspond to highly asynchronous processes, with C−O cleavage far advanced compared to hydrogen atom transfer. To access the chairlike transition state, which has an O−C2−C3−O dihedral angle of 87.5°, only relatively minor adjustments in the more stable pseudodiequatorial ground state conformation, which has a dihedral angle of 77°, are necessary. The calculated activation energy for this process is

(22) Ziegler, F. E. *Chem. Rev.* **1988**, *88*, 1423−1452.

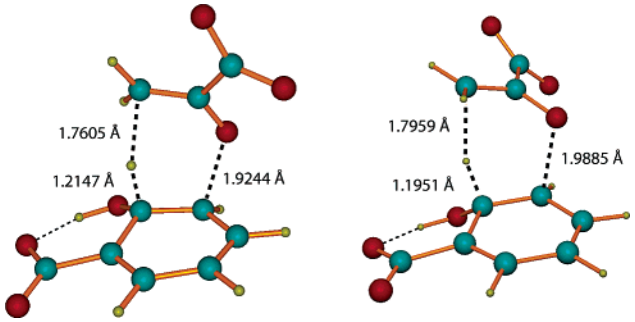

Figure 6. Chairlike (left) and twist boat (right) transition structures for the [1,5]-sigmatropic rearrangement of isochorismate to give salicylate and pyruvate (B3LYP/DZ+(2d,p)). The chair transition state has an O−C2−C3−O dihedral angle of 87.5°, whereas the value for the twist boat is 114.7°.

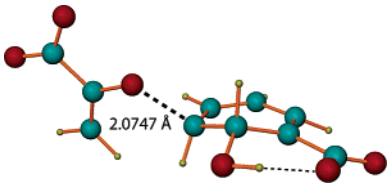

Figure 7. Transition structure for ionization of isochorismate to an ion pair intermediate (B3LYP/DZ+(2d,p)).

25.0 kcal/mol, in good agreement with experiment (26.2 kcal/mol); the predicted ^{2}H isotope effect for the transferred hydrogen atom of 2.071 also agrees well with the experimental value of 2.29 ± 0.11 (Table 1).[23] For comparison, the higher energy twist boat transition state affords a substantially lower isotope effect (1.830). In this case, application of the dielectric continuum model does not alter the intrinsic preference for the chair geometry.

While our calculations support the feasibility of isochorismate decomposing via competitive sigmatropic processes, a fully dissociative pathway, in which rate-determining C−O bond scission affords an ion pair intermediate that subsequently partitions to the observed rearrangement and/or elimination products, represents a conceivable alternative mechanism. The different experimental ^{2}H isotope effects on rearrangement and elimination effectively rule out mechanistic linkage of the two pathways via a common intermediate in this way, but a two-step pathway might apply to either one of the reaction channels alone. A dissociative transition state is expected to be highly unstable in the gas phase due to extensive charge separation. However, we found a region of the potential energy surface where such a species exists, allowing us to estimate the energetics of the ionic pathway. The dissociative structure shown in Figure 7, which is 56.1 kcal/mol higher in energy than the pseudodiequatorial ground state conformer, has a single negative eigenvalue associated with C−O bond scission, but the gradient of this structure is not identically zero because of the flatness of the surrounding energy surface. Application of the dielectric continuum model does not change this estimate much so that the ionic pathway remains more than 20 kcal/mol less favorable than either sigmatropic mechanism. Furthermore, the dissociative

(23) While conventional transition state theory predicts heavy atom isotope effects well (see, for example: (a) Kohen, A. *Prog. React. Kinet. Mech.* **2003**, *28*, 119−156. (b) Scheiner, S. *Biochim. Biophys. Acta* **2000**, *1458*, 28−42. (c) Meyer, M. P.; DelMonte, A. J.; Singleton, D. A. *J. Am. Chem. Soc.* **1999**, *121*, 10865−10874), calculated primary deuterium isotope effects appear to be less accurate. Since higher level variational treatments are currently very difficult, the theoretical isotope effects reported here for the elimination reaction should be viewed with caution.

transition state predicts a deuterium isotope effect of 1.274 at C2, which is substantially higher than the experimental value of 1.06 ± 0.03 observed for the rearrangement and substantially smaller than the experimental value of 2.29 ± 0.11 observed for the elimination. On the basis of these observations, a fully dissociative mechanism appears unlikely for either process.

Discussion

The decomposition modes of isochorismate parallel the uncatalyzed reactions of chorismate, which is another branch-point intermediate in the shikimate biosynthetic pathway as well as the direct precursor of isochorismate (Scheme 3).[1] Like isochorismate, chorismate reacts thermally via competitive rearrangement and elimination pathways, leading to prephenate, on the one hand, and to 4-hydroxybenzoate and pyruvate, on the other.[24]

Although the mechanism of the chorismate transformations has been a matter of some debate, it is clear that the corresponding transition states are relatively polar compared to chorismate based on the effects of substituents[25] and solvent[9] on the reaction rates. However, fully dissociative mechanisms involving a shared ion pair intermediate have been viewed as unlikely.[26] Instead, kinetic isotope effects and computation support concerted but highly asynchronous one-step mechanisms, with considerable C−O bond cleavage at the transition state and comparatively little C−C bond formation (Claisen rearrangement) or hydrogen atom transfer to the enolpyruvyl side chain (elimination).[27]

Our results support similar conclusions for isochorismate (Table 2). The rearrangement and elimination reactions occur with similar rates as their chorismate counterparts, with an 8−9-fold preference for rearrangement over elimination in both cases. The effects of deuterium substitution at the respective alcohol center on both reactions are also comparable. These findings are satisfactorily explained by competing [3,3]- and [1,5]-sigmatropic rearrangements that proceed via different orientations of the enolpyruvyl side chain. Because the reactions involve dianions in solution, they are difficult to characterize theoretically. Nevertheless, the aromatic but asynchronous transition structures with chairlike geometries which are predicted by theory for both rearrangement and elimination afford isotope effects in good agreement with experiment for both chorismate[27] and isochorismate.[23] Although the HDFT calculations incorrectly predict that the elimination reaction of isochorismate should be favored over rearrangement, the small difference in the barriers is within the error of the computational methods.

In nature, the rearrangement reaction of isochorismate has been implicated in the biosynthesis of *m*-carboxy-substituted aromatic amino acids,[2,28] which are produced as secondary metabolites in plants. Although the responsible catalyst has never been isolated, evidence for the enzymatic conversion of isochorismate to isoprephenate has been obtained in crude extracts derived from the plant *Nicotiana silvestria*.[29] By analogy with the reaction catalyzed by chorismate mutase, which accelerates the [3,3]-sigmatropic rearrangement of chorismate to prephenate by more than a million-fold,[24] the name isochorismate mutase was suggested for the putative enzyme.[29] Like its well-studied congener,[27,30] it may exploit a combination of conformational control and electrostatic transition state stabilization to catalyze the Claisen rearrangement of isochorismate.

Salicylate-producing enzymes have been better characterized due to the importance of salicylate in plant defense mechanisms known as local and systemic acquired resistance[31] and because of their role in the biosynthesis of salicylate-based siderophores in several pathogenic bacteria.[32] The conversion of isochorismate to salicylate is catalyzed by the enzyme isochorismate pyruvate lyase (IPL).[33] The enzyme from the opportunistic human pathogen *Pseudomonas aeruginosa*, which is required for the biosynthesis of the siderophore pyochelin, has been studied in some detail.[34,35] It accelerates the elimination reaction by an estimated factor of roughly 4×10^5-fold over the spontaneous thermal process.[36] When [2-^{2}H]isochorismate was employed as a substrate, quantitative transfer of deuterium from C2 to C9 was observed.[37] In addition, a deuterium kinetic isotope effect of 2.34 ± 0.08 on k_{cat} was determined, which is within

Scheme 3. Comparison of the Uncatalyzed Reactions of Isochorismate and Chorismate[a]

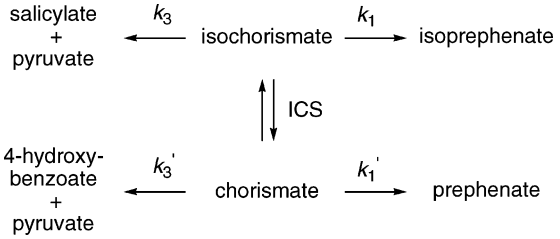

[a] Isochorismate and chorismate are equilibrated by the enzyme isochorismate synthase (ICS).

Table 2. Kinetic Data for Decomposition of Isochorismate and Chorismate[a]

substrate	$10^4 k_1$ (s^{-1})	$^H k_1 / ^D k_1$	$10^4 k_3$ (s^{-1})	$^H k_3 / ^D k_3$
isochorismate	3.63 ± 0.09	1.06 ± 0.03	0.465 ± 0.022	2.29 ± 0.11
chorismate[b]	2.98 ± 0.01	1.07 ± 0.04	0.326 ± 0.009	1.85 ± 0.06

[a] Reactions were carried out in 200 mM sodium phosphate buffer in D_2O (pD 7.5) at 60 °C. [b] Data from ref 27.

(24) Andrews, P. R.; Smith, G. D.; Young, I. G. *Biochemistry* **1973**, *12*, 3492−3498.
(25) (a) Coates, R. M.; Rogers, B. D.; Hobbs, S. J.; Peck, D. R.; Curran, D. P. *J. Am. Chem. Soc.* **1987**, *109*, 1160−1170. (b) Gajewski, J. J.; Jurayj, J.; Kimbrough, D. R.; Gande, M. E.; Ganem, B.; Carpenter, B. K. *J. Am. Chem. Soc.* **1987**, *109*, 1170−1186.
(26) Gajewski, J. J.; Brichford, N. L. *J. Am. Chem. Soc.* **1994**, *116*, 3165−3166.
(27) Wright, S. K.; DeClue, M. S.; Mandal, A.; Lee, L.; Wiest, O.; Cleland, W. W.; Hilvert, D. *J. Am. Chem. Soc.* **2005**, *127*, 12957−12964.
(28) Larsen, P. O.; Onderka, D. K.; Floss, H. G. *Chem. Commun.* **1972**, 842−843; *Biochim. Biophys. Acta* **1975**, *381*, 397−408.
(29) Zamir, L. O.; Nikolakakis, A.; Bonner, C. A.; Jensen, R. A. *Bioorg. Med. Chem. Lett.* **1993**, *3*, 1441−1446.
(30) (a) Chook, Y. M.; Ke, H.; Lipscomb, W. N. *Proc. Natl. Acad. Sci. U.S.A.* **1993**, *90*, 8600−8603. (b) Chook, Y. M.; Gray, J. V.; Ke, H.; Lipscomb, W. N. *J. Mol. Biol.* **1994**, *240*, 476−500. (c) Lee, A. Y.; Karplus, P. A.; Ganem, B.; Clardy, J. *J. Am. Chem. Soc.* **1995**, *117*, 3627−3628. (d) Sträter, N.; Schnappauf, G.; Braus, G.; Lipscomb, W. N. *Structure* **1997**, *5*, 1437−1452.
(31) (a) Wildermuth, M. C.; Dewdney, J.; Wu, G.; Ausubel, F. M. *Nature* **2001**, *414*, 562−565. (b) Durrant, W. E.; Dong, X. *Annu. Rev. Phytopathol.* **2004**, *42*, 185−209.
(32) (a) Marshall, B. J.; Ratledge, C. *Biochim. Biophys. Acta* **1972**, *264*, 106−116. (b) Okujo, N.; Saito, M.; Yamamoto, S.; Yoshida, T.; Miyoshi, S.; Shinoda, S. *Biometals* **1994**, *7*, 109−116. (c) Serino, L.; Reimmann, C.; Baur, H.; Beyeler, M.; Visca, P.; Haas, D. *Mol. Gen. Genet.* **1995**, *249*, 217−228. (d) Pelludat, C.; Brem, D.; Heesemann, J. *J. Bacteriol.* **2003**, *185*, 5648−5653.
(33) This enzyme is encoded by *pchB*, and the protein is thus also referred to as PchB. In addition to IPL activity, PchB also exhibits weak chorismate mutase activity (ref 34).
(34) Gaille, C.; Kast, P.; Haas, D. *J. Biol. Chem.* **2002**, *277*, 21768−21775.
(35) Künzler, D. E.; Sasso, S.; Gamper, M.; Hilvert, D.; Kast, P. *J. Biol. Chem.* **2005**, *280*, 32827−32834.

experimental error of the value of 2.222 predicted for the chairlike elimination transition state at 30 °C, the temperature of the enzymatic experiment.[37] On the basis of this evidence, the IPL-catalyzed reaction, like its thermal counterpart, appears to be pericyclic in nature. How does catalysis occur? Sequence comparisons show that IPL is structurally related to chorismate mutases of the AroQ class; it has even been shown to have low chorismate mutase activity.[34] It is therefore likely that the two enzymes utilize similar mechanistic strategies for accelerating their respective sigmatropic rearrangements,[35] although the relative importance of conformation control versus electrostatic transition state complementarity in the different systems remains an open issue.[38]

Detailed investigations of the structure and mechanism of IPL (and isochorismate mutase) promise to extend our understanding of how enzymes stabilize aromatic transition states. Insights into the isochorismate reaction pathway are also relevant to the chemistry of related shikimate derivatives, including chorismate, 4-amino-4-deoxychorismate, and 2-amino-2-deoxyisochorismate, which undergo similar reactions and serve as building blocks for diverse aromatic metabolites.[1,39] Improved mechanistic understanding of the plant, fungal, and bacterial enzymes responsible for converting these compounds into essential ubiquinones, siderophores, folates, and amino acids will benefit efforts to develop selective herbicides, fungicides, and antibacterial agents.

Acknowledgment. This work was supported by the Schweizerischer Nationalfonds. We are grateful to Professor E. Leistner (University of Cologne, Cologne, Germany) for plasmid pKS3-02, D. Künzler for the generation and characterization of the transformant KA12/pKAD50/pKS3-02, and Professor B. Jaun (ETH Zürich) for expert assistance with the NMR measurements.

Supporting Information Available: Coordinates and computational details for calculation of the theoretical isotope effects, and complete ref 13. This material is available free of charge via the Internet at http://pubs.acs.org.

JA056714X

(36) At 30 °C the k_{cat} value for IPL was determined to be 1.06 s^{-1} (ref 35). Under the same conditions, isochorismate decomposes with an apparent rate constant of $(2.0 \pm 0.5) \times 10^{-5}$ s^{-1} (D. E. Künzler, unpublished). Assuming that the relative rates of the rearrangement and elimination reactions are not strongly temperature dependent, we estimate the rate constant for the uncatalyzed elimination reaction to be approximately $(2.5 \pm 0.6) \times 10^{-6}$ s^{-1}. The acceleration achieved by IPL (k_{cat}/k_{uncat}) is therefore about 4×10^5.

(37) DeClue, M. S.; Künzler, D. E.; Baldridge, K. K.; Kast, P.; Hilvert, D. *J. Am. Chem. Soc.* **2005**, *127*, 15002−15003.

(38) (a) Kast, P.; Grisostomi, C.; Chen, I. A.; Li, S.; Krengel, U.; Xue, Y.; Hilvert, D. *J. Biol. Chem.* **2000**, *275*, 36832−36838. (b) Kienhöfer, A.; Kast, P.; Hilvert, D. *J. Am. Chem. Soc.* **2003**, *125*, 3206−3207. (c) Strajbl, M.; Shurki, A.; Kato, M.; Warshel, A. *J. Am. Chem. Soc.* **2003**, *125*, 10228−10237. (d) Zhang, X. D.; Zhang, X. H.; Bruice, T. C. *Biochemistry* **2005**, *44*, 10443−10448.

(39) Walsh, C. T.; Liu, J.; Rusnak, F.; Sakaitani, M. *Chem. Rev.* **1990**, *90*, 1105−1129.